Design of Phased Arrays in Terms of Random Subarrays

Amit P. Goffer, *Member, IEEE*, Moshe Kam, *Senior Member, IEEE*, and Peter R. Herczfeld, *Fellow, IEEE*,

Abstract—**Analysis and systematic design of uniform phased arrays with subarrays of unequal sizes are absent from the literature, in spite of the appeal of such architectures to wide-bandwidth beam steering. Unequally sized subarrays are expected to outperform identical, contiguous subarrays in terms of array grating lobes. A uniform linear array that is divided into contiguous subarrays of random sizes is studied here. Each array element is connected to a phase shifter, and each subarray is implemented with a common time delayer.**

Closed-form expressions for the average array factor and the variance of the array factor are developed. These expressions enable the formulation of a design procedure that includes the estimation of the peak-grating-lobe level in terms of the probability that the grating lobes will exceed a desired level.

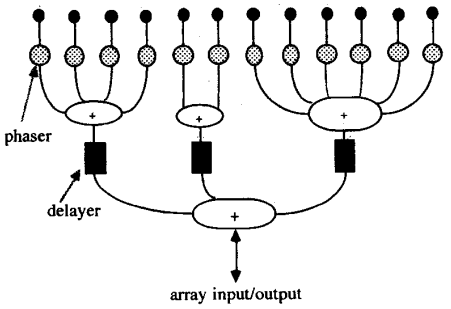

Fig. 1. Random divisions of a 12-element array into contiguous subarrays.

I. Introduction

WIDE-BANDWIDTH beam steering with large phased arrays requires that each element of the array be implemented with a true-time-delay device to avoid beam squinting and broadening. In many applications, this requirement cannot be met because of the size and cost of the delayers, and thus the array is divided into subarrays in order to "save" true-time-delay units and ease the control and computational complexity (see, e.g., [1]). The array is usually divided into contiguous subarrays, identical in size. Each element in the array is fed through a phase shifter (frequency-independent phase-shifting device); each subarray is fed through a common true-time-delay device.

Designs that incorporate contiguous equal size subarrays result in high sidelobes, grating lobes, gain reduction, and squinting in the pointing angle [2], [3] (see also [12], a study of the scanning properties of a subarrayed patch-element infinite array). Sidelobe-level adjustments are often addressed through amplitude tapering; amplitude tapering with uniform illumination within each subarray (amplitude tapering quantization) [2], [4]; or nonuniform illumination within each subarray [5]. *Interlaced* and partially *overlapped* subarray schemes have also been proposed [6] as possible means to allow better grating lobe suppression over a large frequency band, due to a larger (effective) subarray size aperture than the spacing between the subarray centers. Mailloux [1] mentions that reducing the grating lobe peaks in arrays divided into subarrays is possible using subarrays of unequal sizes. This practice tends to reduce peak grating lobes by redistributing the energy into distributed sidelobe regions with lower peak levels, but nearly the same average level. Although overlapped and aperiodic/nonuniform subarraying were reported in the past, no rigorous analysis was presented. Such analysis can provide a methodical design procedure and array performance evaluation.

In this paper, closed form expressions are presented for the average and the variance of the *array factor* of an array divided into contiguous subarrays of random sizes. Based on these expressions, a design procedure is formulated that includes the determination of the range of subarray sizes and the probability of having a specified peak-grating-lobe level. It is shown that the grating-lobe level roughly determines the number of design iterations needed in order to satisfy a required sidelobe level. Moreover, it is possible to estimate the grating-lobe location, level, and gain reduction through the variance behavior.

In all studied configurations, a uniform linear array with $d\lambda_0$ spacing between elements is considered. The number of elements in the kth subarray (the subarray size, M_k) is chosen randomly from a set of equally likely consecutive integers, between $M_{\min}$ and $M_{\max}$. Sizes M_k and M_i are positive integers, statistically independent for $k \neq i$. Since the subarrays are contiguous, the kth *subarray center* I_k is determined according to $I_k = I_{k-1} + \frac{1}{2}(M_{k-1} + M_k)$. I_k is aimed to index the relative location of the kth subarray, thus, it is independent of the element spacing. Fig. 1 demonstrates the studied configuration.

Practical implementation of randomly divided arrays is more complicated than that of a uniformly divided array; it requires nonidentical beamforming networks. However, in many applications, the beamformer may require a small number of network types (if M_k is selected from a small range of values), which for a large array may be a small price for the

Manuscript received July 26, 1993; revised December 2, 1993.

A. P. Goffer is with Elscint Ltd., MRI Division, 550, Haifa 31004, Israel.
M. Kam and P. R. Herczfeld are with the Department of Electrical and Computer Engineering, Drexel University, Philadelphia, PA 19104 USA.

IEEE Log Number 9402817.

better performance (see also [11] for practical realization of a randomly divided array).

A. Random Subarraying versus Randomly Thinned Arrays

We feel that it is worthwhile to emphasize that random subarraying does not serve the same purpose as random-element thinning. Random subarraying, like aperiodic and randomly thinned (or randomly spaced) arrays (see, e.g., [7] and [8]), is performed in order to reduce grating lobes. There are, however, major differences between the random/aperiodic thinned arrays discussed in the literature and the random subarraying analyzed here:

1) The major effort in the area of aperiodic and randomly-thinned arrays was performed for *narrow-bandwidth* applications (where there is no tradeoff between using phasers and delayers); while the method of subarraying was developed for *wide-bandwidth* applications.
2) In the array studied here, the elements are equally spaced. The array is not thinned, and thus it is possible to employ amplitude tapering in addition to subarray size randomization. (Amplitude tapering is practically useless in randomly spaced or thinned arrays.)
3) The aperture may be fully exploited when random subarraying is used, and thus the gain reduction is mostly due to bandwidth and steering angle.
4) In randomly thinned arrays analyzed in the literature (e.g., [7]), the variance of the array factor in the far-from-main-beam region is a constant ($\approx 1/M$, where M is the number of elements), and as a result, the average sidelobe level is $-10\log(M)$. Here the variance and thus the sidelobe level are angle dependent, and from the statistical point of view this is a nonstationary random process. In practice it means that the sidelobe level of the randomly divided array is much more complicated to evaluate than that of the randomly thinned arrays.

The paper is organized as follows. The *average array factor* is defined and computed in Section II. The *variance* of the array factor is calculated in Section III. Design examples of the *CW array factor* (array factor at a single frequency) and the *generalized array pattern* (power pattern for a given instantaneous spectrum) are given in Section IV. Results are compared to those of an array with uniform contiguous identical subarrays. A design procedure is formulated in Section V. We summarize the paper in Section VI.

II. Average Array Factor

The *average array factor*, or the expected value of the array factor, is the outcome of averaging all the possible array factors of a randomly divided array. The average array factor has no grating lobes. The physical array factor (a specific design) would deviate from the average array factor, and thus experience some grating lobes with high probability. It is of interest to determine both the average and the expected deviation from that average, for a specific realization, in order to evaluate the sidelobe level.

The general expression of the array factor of a divided array (without mutual coupling) is (e.g., [1], [2])

$$A(\theta,f)=\sum_{k=-K_1}^{K_1}\frac{\sin\left[M_k\pi d\left(\frac{f}{f_0}u-u_0\right)\right]}{\sin\left[\pi d\left(\frac{f}{f_0}u-u_0\right)\right]}\times\exp\left[j2\pi I_k d\frac{f}{f_0}(u-u_0)\right] \tag{1}$$

where:

$u=\sin(\theta)$ the directional cosine and $u_0=\sin(\theta_0)$,
θ, θ_0: observation and desired pointing angles (with respect to array normal),
M_k: size of the kth subarray, $M_k\in[M_{\min},M_{\max}]$,
I_k: index (location in the array) of the kth subarray center,
K: number of subarrays,
$K_1=\left\{\begin{matrix}K/2 \text{ for even } K\\(K-1)/2 \text{ for odd } K\end{matrix}\right\}$,
d: interelement spacing in wavelengths (at center frequency),
f, f_0: operating and center frequencies.

The first expression on the right hand side of (1) is the array factor of each subarray, which has a maximum at $u=u_p=\frac{f}{f_0}u_0$. The angle squint is due to the fact that each subarray includes phase shifters, which are frequency-independent devices and thus cannot compensate for the time delays that exist because of the impinging wideband signal. The exponent in (1) represents the phase shift due to locations of subarrays, and it depends on the subarray center I_k.

Since the array factor includes a random variable (M_k), *an average array factor* can be defined (similar to randomly thinned arrays [7]), $\overline{A}(\theta,f)=E(A(\theta,f))$, where $\overline{(\cdot)}$ or $E(\cdot)$ is the expected value of $(\cdot)$. The average array factor is computed in the Appendix, part A, and is given by

$$\overline{A}(\theta,f)=A_1\frac{1-A_2^k}{1-A_2}e^{-j\beta/2}, \tag{2}$$

where:

$\alpha=\pi\frac{d\lambda_0}{c}(fu-f_0u_0)$,
$\beta=2\pi d(u-u_0)f/f_0$,
$m=M_{\max}-M_{\min}+1$,
M_s: average subarray size, $E\{M_k\}=M_s$,
M: total number of elements in the array

$$A_1=\overline{\left(\frac{\sin M_k\alpha}{\sin\alpha}e^{jM_k\beta/2}\right)}=\frac{1}{2jm\sin\alpha}\left[e^{jM_s(\alpha+\beta/2)}\frac{\sin\frac{m}{2}(\alpha+\beta/2)}{\sin\frac{1}{2}(\alpha+\beta/2)}-e^{jM_s(\alpha-\beta/2)}\frac{\sin\frac{m}{2}(\alpha-\beta/2)}{\sin\frac{1}{2}(\alpha-\beta/2)}\right]$$

$$A_2=\overline{(e^{jM_k\beta})}=e^{jM_s\beta}\frac{\sin\frac{m}{2}\beta}{m\sin\frac{1}{2}\beta}.$$

In the main beam (α and β are small), $A_1\approx M_s, A_2\approx 1, \frac{1-A_2^K}{1-A_2}\to K$, and thus, $\overline{A}(\theta,f)\approx KM_s$. Far from main beam (sidelobes, $|A_2^K|^2\ll 1$) we have $\overline{A}(\theta,f)\approx\frac{A_1}{1-A_2}$.

The actual array factor will fluctuate about the average array factor of (2). Examining the standard deviation of the actual

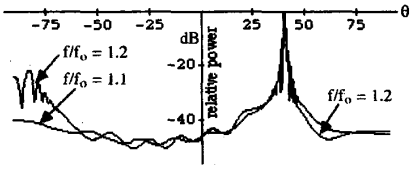

Fig. 2. Average pattern of a randomly divided array: 32 subarrays, the subarry size is uniformly distributed between 2 and 6, steering angle of 40°, $f/f_o = 1.1$ and 1.2.

design from the average array factor, yields an estimate of the grating-lobes peaks. The design may include tapering for additional control of the pattern.

Example 1: The average array factor is calculated for a linear array with $M = 128$ isotropic elements, uniformly $\lambda_0/2$ spaced and divided into 32 subarrays. The average subarray size is $M_s = 4$, and the subarray size is equally likely distributed between $M_{\min} = 2$ and $M_{\max} = 6 (m = 5)$. The subarray center locations are determined according to the random subarray sizes. The steering angle is 40°, and the operating frequencies are $f = 1.1 f_0$ and $1.2 f_0$ (may correspond to a bandwidths of 20% and 40%, respectively).

Fig. 2 shows the square of the average patterns: $[\overline{A}(\theta, f)]^2$ (normalized to the peak of the main beam). For a comparison, Fig. 5 depicts the radiation pattern of a 128-element array, equally divided into 32 contiguous subarrays of four elements each, for a steering angle of 40°. A magnification of these patterns around the pointing angle shows that the main-beam and the close-to-main-beam sidelobes are similar to the uniformly divided or to the undivided arrays. The average pattern does not have grating lobes, since they were eliminated due to the averaging.

III. Variance of the Array Factor

In order to calculate the variance of the array factor, we first compute the average (expected value) of the *power pattern*, $\overline{|A(\theta, f)|^2}$, which is given (see Appendix, part B, for details) by

$$\overline{|A(\theta, f)|^2} = 2\mathrm{Re}\left\{\frac{A_1^2}{1 - A_2}\left[K - 1 - \frac{A_2 - A_2^K}{1 - A_2}\right]\right\} + KA_3, \tag{3}$$

where

$$A_3 = \frac{1}{2\sin^2\alpha}\left(1 - \cos 2\alpha M_s \frac{\sin m\alpha}{m \sin\alpha}\right).$$

In the vicinity of the main beam (α and β are small), $\overline{A(\theta, f)^2} \approx K^2 M_s^2$ (same as in a uniformly divided array with subarray size of M_s). Far from the main beam, ($|A_2^K|^2 \ll 1$) and we have

$$\overline{A(\theta, f)^2} \approx 2\mathrm{Re}\left\{\frac{A_1^2}{1 - A_2}\right\} K + KA_3.$$

The variance of the array factor, $\sigma^2(\theta, f)$, is the difference between the average power pattern and the square of the average pattern, i.e.,

$$\sigma^2(\theta, f) = \overline{|A(\theta, f)|^2} - [\overline{A}(\theta, f)]^2. \tag{4}$$

The variance is important for determining the deviation of the actual pattern from the average array factor, and will enable us later to estimate the grating lobe level. Equation (4) evaluates in the sidelobes region ($|A_2^K|^2 \ll 1$) to

$$\sigma(\theta, f)^2 \approx 2\mathrm{Re}\left\{\frac{A_1^2}{1 - A_2}\right\} K + KA_3 - \frac{|A_1|^2}{|1 - A_2|^2}. \tag{5}$$

Here the variance drops in the vicinity of the pointing angle; the main beam is actually unaffected by the randomization of the subarray size.

A. Peaks of the Variance

It is important to our case to know the location (and the number) of the peaks. These locations correspond to the locations of the *grating-lobe clusters* of any specific design and may be used, as shown later, to estimate the probability that the grating lobes will exceed a specified level. Array parameters such as the range of subarray sizes (m), number of subarrays (K), bandwidth, and gain loss will also be determined. Direct derivation of the variance-peak locations, from (5), is difficult, and though it can be done numerically, we can easily obtain a simple analytical approximation by noticing that most of the grating lobes are caused by the largest subarrays and these grating lobes overlap many of the grating lobes donated by the smaller subarrays. Thus, we can assume that the peaks of the variance appear approximately at angles corresponding to the grating lobes of an array of subarrays, with identical contiguous subarrays of size $M_{\max}$. The array factor of the array of subarrays is given by $(\sin K M_{\max}\beta/2)/(\sin M_{\max}\beta/2)$, so we have grating-lobe clusters at

$$\theta_{\text{grating lobes}} \approx \sin^{-1}\left(u_0 + n\frac{f_0}{dM_{\max} f}\right), n = \pm 1, \pm 2, \cdots. \tag{6}$$

The next example demonstrates that result.

Example 2: The variance of the array from Example 1 is calculated for steering angle of 40°. The normalized variance, $\sigma^2(\theta, f)/M^2$, is plotted in Fig. 3. The peaks of the variance appear at angles according to (6) (substituting $u_0 = \sin 40°$, $M_{\max} = 6$, $f/f_0 = 1.2$, $d = 1/2$ and $n = 1, -1, -2, -3, -4, -5$, yields angles of $67°, 21°, 5°, -10°, -28°, -48°$). The variance drops in the vicinity of the pointing angle, which implies that the main beam does not deviate much from the uniformly divided or undivided array.

The variance can be calculated as a function of frequency f/f_0, subarray size limits m, and steering angle θ_0, as discussed in Section V. For example, since the variance for lower bandwidth is smaller than the variance for higher one (Fig. 3), and the average pattern is smoother (Fig. 2), there will be lower grating-lobe clusters as the bandwidth reduces. The information provided by the variance allows one to predict the deviation of the actual designed radiation pattern from the average pattern. Thus, it is possible to estimate the grating lobes (the probability that the grating lobes exceed a specified value) and the range of subarray size that is required for a specified grating-lobe level.

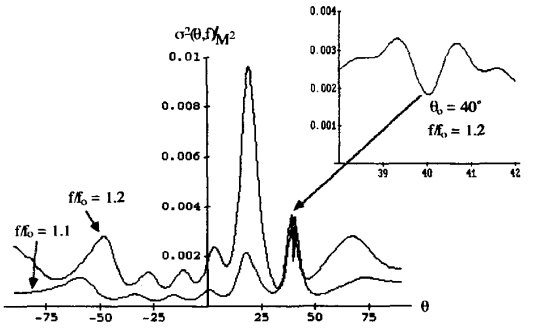

Fig. 3. Variance of the radiation pattern for steering angle of 40°, $M = 128$, $K = 32$, $M_{\min} = 2$, $M_{\max} = 6$, $f/f_o = 1.1$ and 1.2.

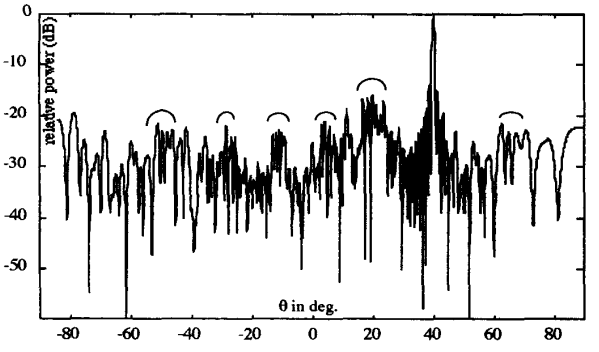

Fig. 4. Design example with random 32 subarrays, $M = 128$, $M_{\min} = 2$, $M_{\max} = 6$, $f/f_o = 1.2$. The markers represent the location of the peaks of the variance (Fig. 3).

IV. Design Example

Power patterns of a 128-element linear array, divided into 32 subarrays, are exemplified for CW (single frequency pattern) and simultaneous bandwidth (generalized power pattern).

A. Single Frequency (CW) Array Factor

The array factor is computed at a single frequency: $f = 1.2f_0$. Fig. 4 depicts the power pattern obtained from a trial with subarray size equally likely chosen between 2 and 6. The subarray sizes are: $\{M_k\} = \{6,3,5,2,\ 4,4,4,6,\ 5,4,3,3,\ 6,2,4,4,\ 5,6,4,4,4,2,3,3,\ 3,5,6,6,\ 6,6,4,3\}$, and the corresponding subarrays centers were computed according to $I_k = I_{k-1} + \frac{1}{2}(M_{k-1} + M_k)$ with $I_1 = 1/2(M_1 - 1)$; $\{I_k\} = \{2.5,7,11,14.5,\ 17.5,21.5,25.5,\ 30.5,36.,40.5,\ 44.,47.,51.5,55.5,\ 58.5,62.5,67.,72.5,\ 77.5,81.5,85.5,88.5,\ 91.,94,97,101,\ 106.5,112.5,118.5,\ 124.5,129.5,133\}$.

Compared to a uniformly divided array (Fig. 5), the grating lobes are suppressed; however, there is a "filling in" of the nulls of the uniformly divided array. Inspecting Fig. 4 reveals *higher sidelobe clusters at angles corresponding to the peaks of the variance* (see Fig. 3). The locations of the clusters maintain a good correspondence to the approximation of (6) (see markers on Fig. 4). This approximation was also verified in additional simulations, and is used in Section V to illustrate

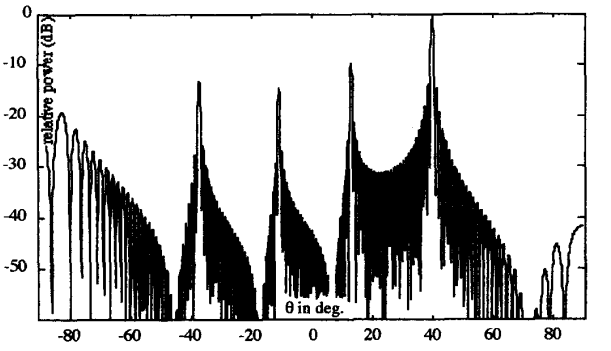

Fig. 5. Pattern of a uniformly divided array, 128 elements divided into 32 subarrays of 4 elements each, steering angle of 40°, $f/f_o = 1.2$.

that the number of the highest peaks in the sidelobe region correspond to the number of the peaks of the variance.

B. Generalized Array Pattern

The radiation pattern of an antenna that is subject to a simultaneous spectrum, $S(f)$, is usually viewed through the *generalized power pattern* (see, e.g., [9], [10]) that is proportional to

$$G(\theta) = \int_{-\infty}^{\infty} \left|A(\theta,f)S(f)\right|^2 df. \tag{7}$$

$G(\theta)$ is relative to the total power at spatial angle of θ. The generalized patterns are exemplified here using a sinc-shaped spectrum: $S(f_i) = \sin\frac{1}{2}\pi\frac{f_i}{f_0}/\frac{1}{2}\pi\frac{f_i}{f_0}$, with $\frac{f_i}{f_0} = 1 + i/8$, $i = 0,\pm1,\cdots,\pm5$ (bi-phase modulated carrier with 3 dB bandwidth of 22%). This spectrum is applied to the array of Examples 1 and 2, and to a uniformly divided array. Fig. 6(a) depicts the generalized pattern of the randomly divided array, and Fig. 6(b) depicts the generalized array pattern of the uniformly divided array. The pointing angle is 40°. Comparing the two array configurations, we note the grating lobes that appear in the uniformly divided array, average out in the case of the randomly divided array.

V. Design Procedure

The variance (5), along with a specified sidelobe level, enables one to determine tradeoffs between various array parameters given a desired level of performance. In what follows, sidelobe peaks and gain loss are estimated, and a design procedure for the various parameters is given.

A. Location and Number of Grating Lobes

Equation (6) gives an estimate of the location and number of the grating-lobe clusters. Substituting $\left|u_0 + n\frac{f_0}{dM_{\max}f}\right| \le 1$, we get

$$-(1+u_0)dM_{\max}\frac{f}{f_0} \le n \le (1-u_0)dM_{\max}\frac{f}{f_0} \tag{8}$$

where n is the (integer) grating lobe number. Let N_{gl} be the *maximum number of grating-lobe clusters*. In our example,

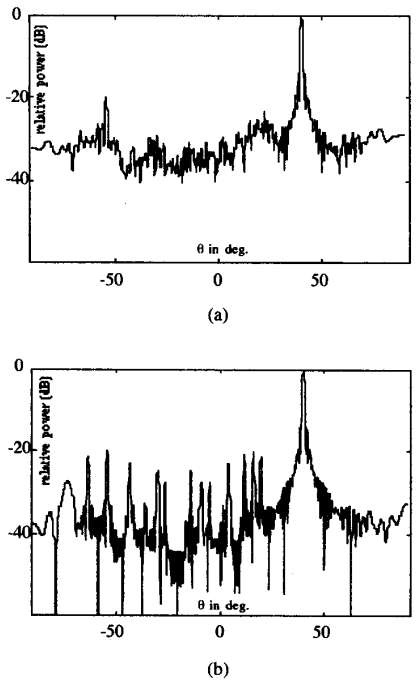

Fig. 6. (a) Generalized power pattern of a randomly divided array. (b) Generalized power pattern of a uniformly divided array.

$u_0 = \sin 40°$, $M_{\max} = 6$, $f/f_0 = 1.2$, $-5.9 \leq n \leq 1.2$, and thus, $N_{\text{gl}} = 6$ ($n = 0$ corresponds to the main beam).

B. Probability of a Single Grating Lobe

Using the variance ((5) or Fig. 3) along with the average pattern ((2) or Fig. 2), we can bound the probability that a single peak will exceed a desired level, through the Tchebycheff inequality:

$$P\{|A(\theta, f) - \overline{A}(\theta, f)| \geq \varepsilon\} \leq \frac{\sigma^2(\theta, f)}{\varepsilon^2} \tag{9}$$

where $P\{\cdot\}$ is the probability of $\{\cdot\}$. Let p_n be the probability that the nth grating lobe exceeds a specified value, and ε be the difference between this desired level and the average pattern; then pn is bounded by the right hand side of (9). ($\sigma^2(\theta, f)$ is the pattern's variance.)

In our example ($m = 5$), the average sidelobe level (at the region corresponding to the grating lobes, but not near the end fire—see Fig. 2) is ≈ -40 dB ($|\overline{A}(\theta, f)| \approx 0.01$). Suppose that the first grating lobe ($n = -1$, $\theta \approx 21°$) is specified to be ≤ -15 dB ($\varepsilon = 10^{-15/20} - 0.01 = 0.1678$), the variance at that point (Fig. 3, $\theta \approx 21°$) is 0.00965, and thus the probability that the first grating lobe, p_{-1}, will exceed this level is $p_{-1} \leq 0.00965/0.1678^2 = 0.34$. As for the rest of the grating-lobe clusters, the variance ≈ 0.003, which yields $p_n \leq 0.37$ for a desired level of -20 dB ($n = 1, -2, -3, -4, -5$).

C. Grating-Lobe Estimation: Probability of the Grating Lobes

The next step is to calculate the probability that the grating lobes exceed a specified level. This is done through (9). Let P_N be the probability that N grating-lobe clusters (out of the total number N_{gl}) exceed a specified level, and let P_{gl} be the probability that at least one grating-lobe cluster exceeds a specified level. An approximation to P_N and P_{gl} can be calculated, under the following assumptions:

1) The (random) grating-lobe peaks are approximately statistically independent.
2) The probabilities that the grating-lobe clusters exceed the specified level are equal, i.e., $p_n = p$, $\forall n$. (Alternatively, the largest p_n can be chosen as p.)
3) The grating-lobe peaks are higher than the rest of the sidelobes.

Assumption 1 results from the following argument. The grating lobes are originated by the *array of subarrays*, i.e., the array that is constituted by the centers of the subarrays. This is a *randomly thinned array*, and samples of its pattern can be considered as independent provided the intervals between the samples are large enough [7]. Under these assumptions, P_N is given by the binomial distribution function

$$P_N = p^N (1-p)^{N_{\text{gl}} - N} \binom{N_{\text{gl}}}{N}. \tag{10}$$

The probability P_{gl} that at least one grating lobe surpasses a specified level is the summation over all the grating lobes possibilities, i.e., $P_{\text{gl}} = \sum_{N=1}^{N_{\text{gl}}} P_N$, and since $\sum_{N=0}^{N_{\text{gl}}} P_N = 1$, we have

$$P_{\text{gl}} = 1 - (1-p)^{N_{\text{gl}}}, \tag{11}$$

which is a monotonically increasing function of the probability of a single grating-lobe cluster, p. An *upper bound* is obtained if we select $p = \sigma^2(\theta, f)/\varepsilon^2$ and we have

$$P_{\text{gl}} \leq 1 - \left(1 - \frac{\sigma^2}{\varepsilon^2}\right)^{N_{\text{gl}}}. \tag{12}$$

Equation (12) gives an upper-bound estimate (in probability) to the number of design iterations required in order to achieve a desired specified sidelobe level. In our example, the probability that at least one of the grating lobes (not including the grating lobe adjacent to the main beam, $n = -1$) will exceed -20 dB ($p = 0.37$, $N_{\text{gl}} = 5$) is ≤ 0.90. The interpretation is that out of ten design tries at least one on average is expected to comply with the requirement of -20 dB. Numerous design examples have been simulated for this study, and this prediction was confirmed.

D. Gain Loss

Gain loss can be estimated using (9) and assuming that the area under the sidelobes is approximately constant for various designs (with same design parameters). The gain loss is demonstrated here using Example 2 (Section III, Fig. 3). The variance at the pointing direction is $\sigma^2(\theta_0 = 40°, f = 1.2f_0) \approx 0.0018$. Equation (9) yields an upper bound to the probability that the gain loss will exceed a certain level, as demonstrated in the next table:

Gain Reduction $\geq$		with Probability $\leq$
1/2 dB	($\varepsilon = 0.056$)	57%
1 dB	($\varepsilon = 0.1$)	15%
2 dB	($\varepsilon = 0.2$)	4%

Thus we have a relatively high probability that a random design will introduce a gain loss that is smaller than 0.5 dB, and a relatively low probability that a gain loss exceeds 1 dB. In all the design examples simulated for this study (using the same M, M_s, m, f/f_0, and θ_0), these results were confirmed.

E. Subarray Size and Bandwidth Considerations

The range of the subarray size ($M_{\max} - M_{\min} = m - 1$) and the desired bandwidth can be determined as follows.

1) Decide upon a "reasonable" P_{gl} (probability that at least one grating-lobe cluster will exceed a specified level). This decision involves a tradeoff; in our example, $P_{\text{gl}} = 99.9\%$ corresponds to grating lobes of -23 dB, and it is reasonable to have hundreds of design iterations before getting the desired response. For $P_{\text{gl}} = 90\%$, we got -20 dB after few simulation iterations.
2) Obtain N_{gl} (number of grating-lobe clusters or variance peaks) from (8).
3) Derive the ratio σ^2/ε^2 from (12). $(1 - (1 - P_{\text{gl}}^{1/N_{\text{gl}}} \rightarrow \sigma^2/\varepsilon^2.)$
4) Given the maximum desired grating-lobe level, obtain ε^2 using (2) or Fig. 2 (ε is the difference between this desired level and the average pattern). Obtain the desired variance, σ^2, from step 3.
5) Desired array parameters can now be obtained. Using the desired σ^2 of step 4 (which is the maximal allowed value for the variance), plot the variance (5) versus θ with m (or f/f_0) as a parameter; the desired parameter (m or f/f_0) is the one that complies with the desired σ^2.

VI. Summary

The closed-form analysis of a randomly divided array presented here enables a rigorous design of a low grating-lobe wideband array. Expressions for the average array factor and variance of the array factor were derived. Based on these expressions, a design method was demonstrated through which the grating lobes and the gain loss can be estimated, namely: location and number of grating-lobe clusters, probability that the grating lobes will exceed a specified level, and probability of having a specified gain loss. The various array parameters (subarray sizes, bandwidth, and maximum steering angle) can be determined through the design process.

Appendix

A. Average Array Factor

Rewriting (1) with the symbols used in (2) we get

$$A(\theta, f) = \sum_{k=-K_1}^{K_1} \frac{\sin(M_k\alpha)}{\sin(\alpha)} e^{jI_k\beta} \tag{A-1}$$

where $\alpha = \pi d(\frac{f}{f_0}u - u_0)$ and $\beta = 2\pi d\frac{f}{f_0}(u - u_0)$. We substitute into (A-1) the relation of the random subarray sizes to the subarray locations: $I_k = I_{k-1} + \frac{1}{2}(M_{k-1} + M_k)$, with $I_1 = 1/2(M_1 - 1)$, and we get

$$\overline{A}(\theta, f) = e^{-j\beta/2} \sum_{k=1}^{K} \overline{\left(\frac{\sin M_k\alpha}{\sin\alpha} e^{jM_k\beta/2}\right)} \times \overline{(e^{jM_{k-1}\beta})(e^{jM_{k-2}\beta})} \cdots \overline{(e^{jM_1\beta})}. \tag{A-2}$$

Using $\overline{(\cdot)} = \frac{1}{m}\sum_{M_{\min}}^{M_{\max}}(\cdot)$ and defining A_1 and A_2 as in (2), we get $\overline{A}(\theta, f) = e^{-j\beta/2}\sum_{k=1}^{K} A_1 A_2^{k-1}$, which results in (2).

B. Average Power Pattern

Using (1), the square of the absolute value of the array factor is given by

$$|A(\theta, f)|^2 = \frac{1}{\sin^2\alpha} \sum_k \sum_n \sin(M_k\alpha)\sin(M_n\alpha) e^{jI_k\beta} e^{-jI_n\beta}. \tag{B-1}$$

Substituting the relation

$$(I_k - I_n) = \begin{cases} \frac{1}{2}[M_k + M_n] + [M_{n+1} + \cdots + M_{k-1}] & \text{for } k > n \\ -\frac{1}{2}[M_k + M_n] - [M_{k+1} + \cdots + M_{n-1}] & \text{for } k < n \end{cases}$$

into (B-1) yields

$$\begin{aligned} |A(\theta, f)|^2 = {} & \sum_{k=2}^{K}\sum_{n=1}^{k-1} \left(\frac{\sin M_k\alpha}{\sin\alpha}\right)\left(\frac{\sin M_n\alpha}{\sin\alpha}\right) \\ & \times \operatorname{Exp}\left\{j\beta\left[\frac{1}{2}(M_k + M_n) + (M_{n+1} + \cdots + M_{k-1})\right]\right\} \\ & + \sum_{n=2}^{K}\sum_{k=1}^{n-1} \left(\frac{\sin M_k\alpha}{\sin\alpha}\right)\left(\frac{\sin M_n\alpha}{\sin\alpha}\right) \\ & \times \operatorname{Exp}\left\{j\beta\left[\frac{1}{2}(M_k + M_n) - (M_{k+1} + \cdots + M_{n-1})\right]\right\} \\ & + \sum_{k=1}^{K}\left(\frac{\sin M_k\alpha}{\sin\alpha}\right)^2. \end{aligned} \tag{B-2}$$

The first term in (B-1) corresponds to $k > n$, the second corresponds to $k < n$, and the third corresponds to $k = n$. The expectation over $|A(\theta, f)|^2$ gives

$$\begin{aligned} \overline{|A(\theta, f)|^2} = {} & \sum_{k=2}^{K}\sum_{n=1}^{k-1} \overline{\left(\frac{\sin M_k\alpha}{\sin\alpha} e^{j\frac{1}{2}\beta M_k}\right)} \\ & \times \overline{\left(\frac{\sin M_n\alpha}{\sin\alpha} e^{j\frac{1}{2}\beta M_n}\right)} \\ & \times \overline{(e^{j\beta M_{n+1}})} \cdots \overline{(e^{j\beta M_{k-1}})} \\ & + \sum_{n=2}^{K}\sum_{k=1}^{n-1} \overline{\left(\frac{\sin M_k\alpha}{\sin\alpha} e^{-j\frac{1}{2}\beta M_k}\right)} \\ & \times \overline{\left(\frac{\sin M_n\alpha}{\sin\alpha} e^{-j\frac{1}{2}\beta M_n}\right)} \\ & \times \overline{(e^{-j\beta M_{k+1}})} \cdots \overline{(e^{-j\beta M_{n-1}})} \\ & + \sum_{k=1}^{K}\overline{\left(\frac{\sin M_k\alpha}{\sin\alpha}\right)}^2. \end{aligned} \tag{B-3}$$

Defining $A_3 \overline{\left(\frac{\sin M_k\alpha}{\sin\alpha}\right)}^2 = \frac{1}{2\sin^2\alpha}\left(1-\cos 2\alpha M_s \frac{\sin m\alpha}{m\sin\alpha}\right)$, and using A_1, A_2 (defined in (2)) gives

$$\overline{|A(\theta,f)|^2} = \left[A_1^2 \sum_{k=2}^{K}\sum_{n=1}^{k-1} A_2^{k-n-1}\right] + \left[A_1^2 \sum_{k=2}^{K}\sum_{n=1}^{k-1} A_2^{k-n-1}\right]^* + KA_3, \quad \text{(B-4)}$$

where $[\cdot]^*$ denotes complex conjugation. Equation (B-4) leads directly to (3).

REFERENCES

[1] R. J. Mailloux, "Phased array theory and technology," *Proc. IEEE*, vol. 70, no. 3, pp. 246–291, Mar. 1982.

[2] ——, "Array grating lobes due to periodic phase, amplitude, and time delay quantization," *IEEE Trans. Antennas Propagat.*, vol. AP-32, no. 12, pp. 1364–1368, Dec. 1984.

[3] R. L. Howard *et al.*, "The relationships between dispersion loss, sidelobe level, and bandwidth in wideband radar with subarrayed antennas," in *Proc. IEEE Int. Symp. Antennas and Propagation*, vol. 1, pp. 184–187, 1988.

[4] K. S. Rao and I. Karlsson, "Low sidelobe design considerations of large linear array antennas with contiguous subarrays," *IEEE Trans. Antennas Propagat.*, vol. AP-35, no. 4, pp. 361–366, Apr. 1987.

[5] R. L. Haupt, "Reducing grating lobes due to subarray amplitude tapering," *IEEE Trans. Antennas Propagat.*, vol. AP-33, no. 8, pp. 846–850, Aug. 1985.

[6] R. Tang, "Survey of time-delay beam steering techniques," in *Phased Array Antennas*, A. A. Oliner and G. H. Knittel, Eds. Bedham, MA: Artech, 1972, pp. 254–260.

[7] B. D. Steinberg, *Principles of Aperture and Array System Design*. New York: Wiley, 1976, pp. 123–167.

[8] M. G. Sharma and G. S. Sanyal, "Position-modulated phased array—space factor considerations," *IEEE Trans. Antennas Propagat.*, vol. AP-27, no. 3, pp. 373–378, May 1979.

[9] C. B. Sharpe and R. B. Crane, "Optimization of linear arrays for broadband signals," *IEEE Trans. Antennas Propagat.*, vol. AP-14, no. 4, pp. 422–427, July 1966.

[10] J. Frank, "Bandwidth criteria for phased array antennas," in *Phased Array Antennas*, A. A. Oliner and G. H. Knittel, Eds. Bedham, MA: Artech, 1972, pp. 243–253.

[11] I. Groger, W. Sander, and W.-D. Wirth, "Experimental phased array radar ELRA with extended flexibility," *IEEE AES Mag.*, pp. 26–30, Nov. 1990.

[12] D. M. Pozar, "Scanning characteristics of infinite arrays of printed antenna subarrays," *IEEE Trans. Antennas Propagat.*, vol. 40, no. 6, pp. 666–674, June 1992.

Amit P. Goffer (M'91) received the B.Sc. degree in electrical engineering from the Technion, Haifa, Israel, in 1975, the M.Sc. degree in electrical engineering from Tel-Aviv University, Tel-Aviv, Israel, in 1984, and the Ph.D. degree from Drexel University, Philadelphia, PA, in 1990.

From 1975 to 1980 he was with the Israeli Defense Forces, working on communication techniques and systems. In 1980 he joined Rafael, Israel, where he worked in the field of adaptive arrays. From 1988 to 1991 he was at Drexel University, where he carried out research on phased arrays, focusing on wideband applications. In 1991 he joined Elscint, Israel, where he is now the Magnetics Department Manager in the MRI Division.

Dr. Goffer is the recipient of the Rafael Award and a member of Sigma Xi.

Moshe Kam (S'75–M'77–S'83–S'85–M'86–SM'92) received the B. Sc. degree from Tel-Aviv University, Tel-Aviv, Israel, in 1977, and the M.S. and Ph.D. degrees from Drexel University, Philadelphia, PA, in 1985 and 1987, respectively.

Between 1976 and 1983 he was a Technical Officer with the Israeli Defense Forces. Since 1986 he has been on the faculty of Drexel University, where he is now the Director of the Data Fusion Laboratory (DFL) and an Associate Professor. He investigates large-scale systems and distributed-detection architectures, and he has written extensively about decision fusion and multisensor systems. His findings were applied to the design of pattern-recognition modules and robotic systems at the DFA, and to applications in power-system control, multiaccess communications, and forensic science.

Dr. Kam was a recipient of a NSF Presidential Young Investigator award (1990) and of the Eta Kappa Nu C. Holmes MacDonald Award (1991). He is an associate editor of the IEEE TRANSACTIONS ON SYSTEMS, MAN, AND CYBERNETICS and of *Pattern Recognition*.

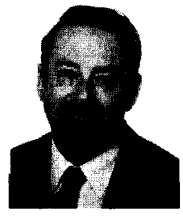

Peter R. Herczfeld (S'66–M'67–SM'89–F'91) received the B.S. degree in physics from Colorado State University in 1977, and the M.S. degree in 1963 and the Ph.D. degree in 1967, both from the University of Minnesota, Minneapolis.

Since 1986 he has been on the faculty of Drexel University, where he is now a Professor and the Director of the Microwave-Lightwave Engineering Center. The Center is committed to timely and original research in microwaves and photonics.

Dr. Herczfeld has authored more than 300 papers in solid-state electronics, microwaves, photonics, solar energy, and biomedical energy, and has served as project director for more than 70 projects. he is the recipient of several research and publication awards, including the *Microwave Prize*, He is a member of APS, SPIE, and ISEC.